MECHANICAL PROPERTIES ENHANCEMENT OF BORON CARBIDE BASED ARMOUR MATERIALS

Priyadi Hartoko
Indonesian Navy & University of New South Wales
School of Materials Science and Engineering, UNSW Sydney, Australia 2052
priyadi.hartoko@student.unsw.edu.au

Sean Li
University of New South Wales
School of Materials Science and Engineering, UNSW Sydney, Australia 2052
sean.li@unsw.edu.au

Article Info

Abstract

Lightweight armor materials made from ceramics have become a great interest in the past decades. There have been many research efforts to develop the high-performance ceramics for this particular application. Boron carbide (B_4C) is one of the promised candidates due to its extraordinary hardness, wear resistance, chemical inertness, ultra-lightweight, and its high resistance to radiation. However, the strong covalent bonding nature of B_4C makes it hard to be sintered. Sintering at high temperatures and the presence of impurities can also result in grain coarsening. One of the methods being used to overcome the problems is to introduce Boron (B) as a sintering aid into raw materials of B_4C. To evaluate the effects of B addition on the sinterability of B_4C, B_4C powders were ball-milled with B powders in different ratios and the mixtures of B_4C and B were processed by spark plasma sintering technique. Density and toughness of the as-sintered materials were increased along with increasing B content in the range from 1 wt% to 7 wt% while hardness and strength of the samples were also increased when the percentage of B addition is up to 5 wt%.

INTRODUCTION

Boron carbide (B_4C) is widely known as one of the hardest materials in nature, its hardness comes third only after diamond and c-boron nitride. Besides its high hardness (29-35 GPa), B_4C also has other outstanding properties such as high wear resistance, good chemical inertness in a corrosive environment, very low density (2.52 g/cm^3), a high cross-section for neutron absorption, and high resistance to radiation. With all advantages that come from its properties, B_4C has been used for armor, abrasive materials, wear-resistant components, and parts in nuclear industries (Chen, McCauley, & Hemker, 2003; M. W. Chen, McCauley, LaSalvia, & Hemker, 2005; Emin & Aselage, 2005; Roy, Subramanian, & Suri, 2006; Thévenot, 1990). Despite the fact that B_4C seems to be a promising material with its properties, there are some shortcomings as well because of its other properties. B_4C's strong covalent bond makes it hard to sinter into full theoretical density, sintering at high temperature and the presence of oxide as well as free carbon can also trigger grain coarsening which decreases its mechanical properties. Besides that, B_4C's low fracture toughness also limits its application (M. W. Chen et al., 2005; Lee, Speyer, & Hackenberger, 2002; Roy, Subramanian, Suri, 2006; Thévenot, 1990).

Spark Plasma Sintering (SPS) technique has become one solution to process dense B_4C samples with relatively lower temperatures and shorter holding times if compared to other conventional techniques, due to its pulsed direct current and uniaxial pressure applied during the sintering process. SPS also involves a controlled heating rate, one of its advantages to mitigate possibilities of grain growth during sintering (Chaim, 2016; Hitchcock, Livingston, & Liebenberg, 2015; Shen & Nygren, 2005; Zhang et al., 2014).

Elemental boron (B) is one of the established sintering aids for many different powder metallurgies of steel alloys and ceramics. The use of sintering aids has different purposes, some added to make the sintering temperature lower, while others added to hinder grain growth. Some added to introduce residual stress because of thermal shock resistance and change the oxidation rate as well. In B_4C sintering process, since free carbon is one of the impurities that hinder densification, B is added into the matrix to eliminate excess free carbon (B. Champagne, 1979; Bakan, Heaney, & German, 2001; Liu, Cardamone, Potter, German, & Semel, 2000; Cabral Miramontes, Barceinas Sánchez, Almeraya Calderón, Martínez Villafañe, & Chacón Nava, 2010; Luo, Yang, Schaffer, & Qian, 2013).

Although there have been some efforts to increase B_4C sinterability in the SPS process by adding different sintering aids, reports on the effect of elemental boron used as a sintering aid in B_4C powder metallurgy are very limited. Hence in this paper, B_4C powders were mixed with different amounts of elemental B powders to evaluate the effects of the mixtures, the sintering process of the mixed powders, and explain changes in B_4C properties because of the addition.

METHODS

Experimental Procedures

B_4C powders used as starting materials were obtained from Mudanjiang Jingangzuan Boron Carbide Co. Ltd., Mudanjiang, China. While elemental B powders were obtained from Sigma-Aldrich Pty Ltd. Particle size analysis for B_4C and B powders was performed by a laser particle sizer Malvern Zetasizer 3000 with the *d50* size of 1.72 µm and 12.1 µm, respectively. The morphologies of both powders are shown in Figure 1 and 2.

To achieve a better degree of dispersion, B_4C and B powders were wet ball-milled with pure ethanol as a solvent and WC milling balls in 1:4 powder to ball ratio. Various amounts of B were added to B_4C powders, from 1 wt% to 7 wt%, and
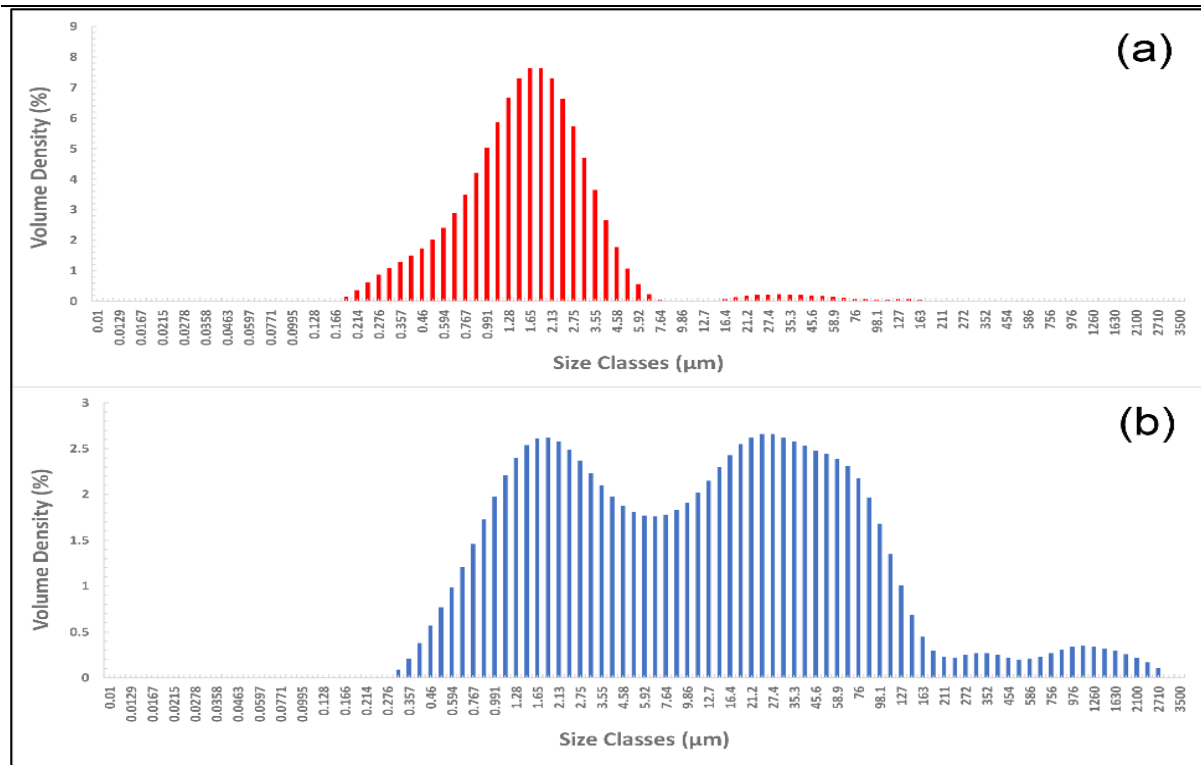
Figure 1. Size distribution of B$_4$C (a) and B (b) powders
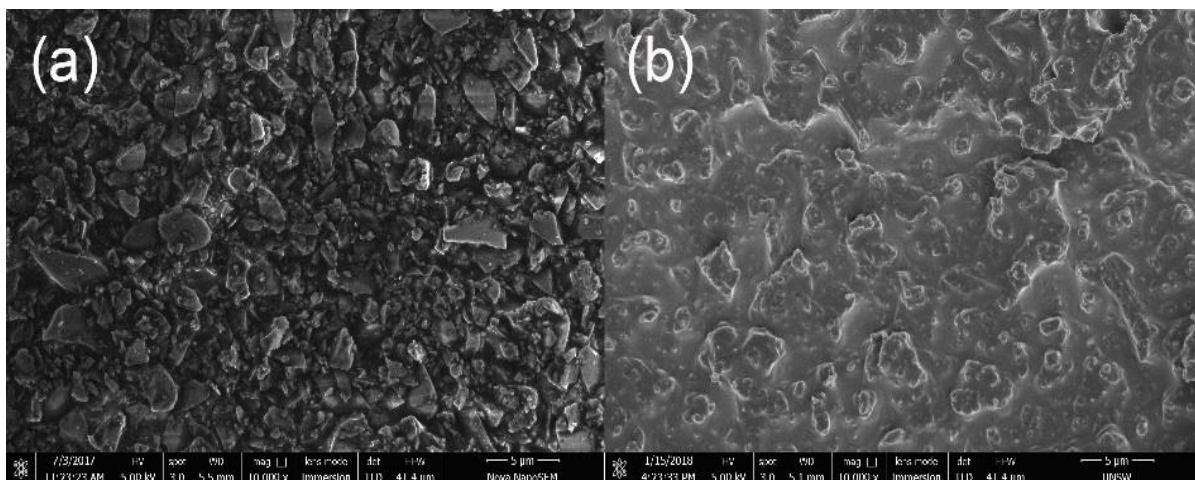*Source:* Processed by Authors, 2020.

Figure 2. The appearance of B$_4$C (a) and B (b) powders
Source: Processed by Authors, 2020.

ball-milled for 24 hours at 250 rpm. After being dried in the air, the mixtures were sieved through a 560 µm mesh sieve and put into a 110 ˚C drying oven for 5 hours.

The dried powders were put into cylindrical graphite die with an inner diameter of 50 mm, pre-pressed to compact the powders, and sintered under vacuum in a Dr. Sinter 8000 (SPS Syntex Inc., Japan) SPS apparatus under a pressure of 40 MPa which was applied all the time. Sintering temperature and holding times for all the experiments were 1900 ˚C and 5 minutes, respectively, while a 12 ms/on and 2 ms/off pulsed direct current were used during the process. The apparatus was set to a rapid heating rate of 100˚ C/min, and to measure the
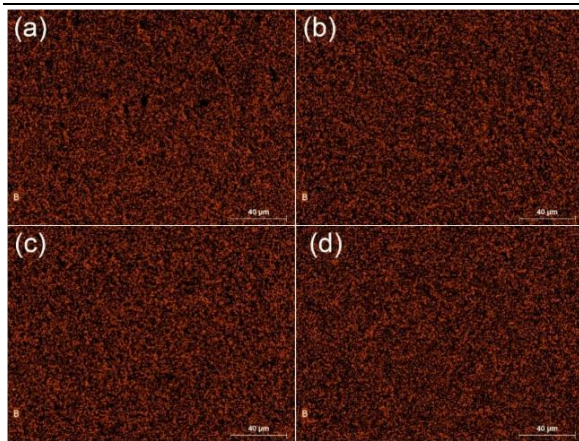
Figure 3. EDS/ EDX mapping of the samples with 1 wt% (a), 3 wt% (b), 5 wt% (c), and 7 wt% (d) of elemental B
Source: Processed by Authors, 2020.

Figure 4. XRD patterns of the polished samples
Source: Processed by Authors, 2020.

temperature, a Chino Radiation Thermometer (IR-AH) was used and being focused on a small hole in the die.

The crystalline phase identifications were performed by X-ray diffractometry (Philips X'pert Pro MPD) and analyzed with HighScore Plus software. The porosity of the samples was calculated by the Archimedes method according to the ASTM C20-00 standard.

The powder's and sample's microstructural characterizations and Energy Dispersive X-Ray Spectroscopy (EDS/ EDX) analysis were carried out by field-emission scanning electron microscope (FEI Nova Nano SEM 230 and 450), while the sample's Vickers hardness values were determined using Struers DuraScan Vickers microhardness tester with a pyramidal diamond indenter and a load (P) of 1 kg for 15 seconds. Fracture toughness of the samples was determined from Palmqvist to crack emanated from the indenter, while flexure strengths were obtained by 3-point-bend tests using Instron 5565 equipment with 20mm fulcrum spacing and a crosshead speed of 0.5 mm/min.

RESULTS AND DISCUSSION

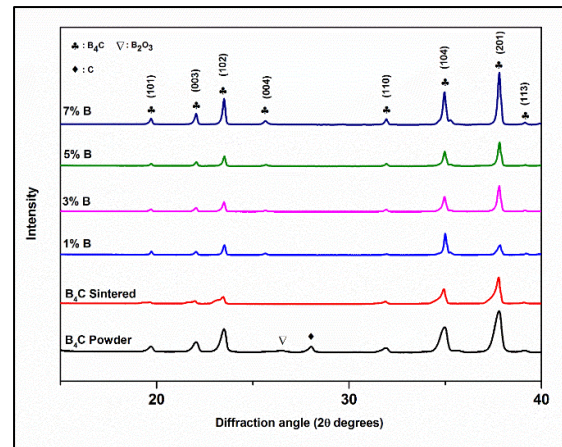The EDS/ EDX mapping of elemental B on each of the samples can be seen in Figure 3 and showed that elemental B can be dispersed uniformly throughout the samples. The analysis proved that the wet ball-milling method is an effective way to mix elemental B and B_4C powders. X-ray diffraction patterns were plotted to analyze sample's phase composition after consolidated in the SPS. The patterns were shown in Figure 4, with its diffraction angles were restricted from 20° to 40° to highlight important peaks.

It can be seen from the graphs that the free carbon amount in the B_4C powders was eliminated once the powders sintered and we can see that there is a new B_4C phase formed at the angle of 25,7°. Furthermore, as B quantities getting larger in each of the sample groups, B_4C peaks intensities are getting higher. The patterns are consistent with the results of other experiments which confirm that the excess amount of B can react with free carbon impurities in the B_4C powders to form B_4C phase (Larsson, Axén, & Hogmark, 2000).

Since most of the free carbon impurities that hinder densification can be removed, the densification process during sintering can be performed better hence porosity of the samples can be reduced as the amount of B getting larger. The porosity of the samples without sintering additives was recorded at the value of 1.49% and can be reduced up to 0.87% in the samples with 7 wt% B additives. This confirms the

23

previous observation done by other researchers (Bouchacourt, M., Brodhag, C., & Thevenot, 1981) and (Bouchacourt & Thevenot, 1981). Surface analysis of the samples performed by scanning electron microscopy in this work supports the theory as well. As can be seen from the SEM images in Figure 5, surface porosities were decreasing as the additive amount in the matrices become larger.
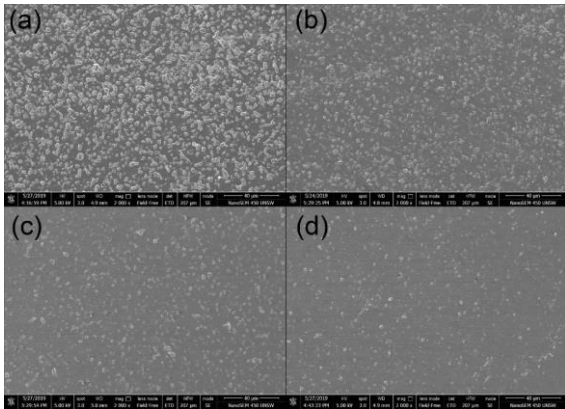

Figure 5. Surface porosities of the samples with 1 wt% (a), 3 wt% (b), 5 wt% (c), and 7 wt% (d) of elemental B
Source: Processed by Authors, 2020.

Samples with only 1 wt% B additives have pores throughout their surfaces. The pores are relatively big and interconnected, making the overall density low. As the amount of B additives becomes larger in the mixtures, the sintered samples are having fewer pores. It can be seen from the surfaces of the samples with 7 wt% B additives, the pores that can be seen are mostly micro ones hence the degree of the overall density is much higher.

Figure 6 and Table 1 summarizes the properties obtained from the samples analyzed in this work. As the porosity of the samples decreasing with a larger B amount, the samples getting dense hence their fracture toughness trend is increasing. The porosity of the samples without sintering aid was recorded as 1.49% and can be reduced to only 0.87% with the addition of 7 wt% elemental B powders. The value of the fracture toughness can be increased up to 3.33 MPa.$\sqrt{m}$ from the

value of 2.58 MPa.$\sqrt{m}$ in the sample without sintering aid. The elevated fracture toughness follows a linear trend as the amount of elemental B powders increased from 1 wt% to 7 wt%.

Ceramic materials are highly brittle in nature, they do not have dislocation mobility as found in metals since ceramics have different atomic bonds. Ceramics processing by sintering at high temperatures also left undesired pores and structural imperfections (Reed, 1994; W.D. Kingery, H.K. Bowen, 1975). The level of porosity affects fracture toughness since porosity is one of the sources of crack initiation, hence reducing porosities is one of the primary methods to mitigate the occurrence of crack propagations. This relation explains why fracture toughness is increasing as the porosity decrease with a larger sintering aid amount.

Hardness and flexural strength of the samples tend to increase as the amount of B getting larger until at some points they reached maximum values then decreases as the additives become larger. Pure B_4C sample has 30.29 GPa hardness and with the addition of 5 wt% B can be increased to 32.93 GPa, but it decreased to 31.78 with larger 7 wt% of B additives.

Our results on the flexure strength showed that it can be elevated from 213.7 MPa at the samples without sintering aids to the highest of 419.3 MPa at the samples with addition of 5 wt% B and decreased to 309.9 Mpa as the amount of the additives become 7 wt%.

The maximum values of hardness and flexure strength can be seen in the samples with 5 wt% B and the increasing trends were due to the facts of the decreasing porosity in the samples. However, although the porosities of the samples are still decreasing on the samples with 7 wt% of B addition, their hardness and flexure strength values are lower. It is hypothesized that the reducing values of hardness and flexure strength in the samples that are having more than 5 wt% B are caused by altered B_4C stoichiometry

because of the excess B in the matrices. Difference stoichiometry gives different atoms arrangements and their bonds hence affect the material's properties.

CONCLUSIONS

The addition of elemental boron as a sintering aid for B_4C was meant to eliminate free carbon impurities. With the impurities eliminated, the densification process during high-temperature sintering can occur more easily, the porosity of the samples can be reduced, hence it improves B_4C's fracture toughness. Besides fracture toughness, the addition elevates other properties as well, i.e. hardness and flexure strength, to a certain point when the values reached its maximum point then decreased as the amount of the additives become larger. In the case of the reducing values of hardness and flexure strength after maximum points, excess amount of elemental B as a sintering aid in the matrices is hypothesized as a cause in altering B_4C's stoichiometry, hence there are differences in the material's final properties.

The results of this work show that elemental B can be used and become one of the options for B_4C sintering aids, concerning certain preferred properties and the amount of the additives being added. In this work, the lowest porosity and the highest fracture toughness values which are 0.87% and 3.33 MPa.√m, respectively, can be obtained by mixing 7 wt% of elemental B into the B_4C matrices. However, concerning the sample's hardness and flexural strength, the maximum values of 32.93 GPa (hardness) and 419.3 MPa (flexural strength) were recorded from samples with 5 wt% of elemental B addition.

The experiments in this work showed that the amount of sintering aid added to the mixtures needs to be considered properly to achieve the desired properties. Although adding a certain amount of the sintering aid has positive effects on one or more properties, it does not necessarily give the same result for the others. The optimum amount of the sintering aid added is preferred to deliver the best possible outcomes.

ACKNOWLEDGMENTS

REFERENCES

B. Champagne, R. A. (1979). Mechanical properties of hot-pressed B-B4C materials. *Journal of the American Ceramic Society*, *62*(3–4), 149–153.

Bakan, H. I., Heaney, D., & German, R. M. (2001). Effect of nickel boride and boron additions on sintering characteristics of injection moulded 316L powder using water soluble binder system. *Powder Metallurgy*. https://doi.org/10.1179/0032589016 66392

Bouchacourt, M., Brodhag, C., & Thevenot, F. (1981). Hot Pressing of Boron and Boron Rich Compounds: B6o, B10.5c-B4c. In *Science of Ceramics*.

Bouchacourt, M., & Thevenot, F. (1981). The properties and structure of the boron carbide phase. *Journal of The Less-Common Metals*. https://doi.org/10.1016/0022-5088(81)90223-X

Cabral Miramontes, J. A., Barceinas Sánchez, J. D. O., Almeraya Calderón, F., Martínez Villafañe, A., & Chacón Nava, J. G. (2010). Effect of boron additions on sintering and densification of a ferritic stainless steel. *Journal of Materials Engineering and Performance*. https://doi.org/10.1007/s11665-009-9544-1

Chaim, R. (2016). On densification mechanisms of ceramic particles during spark plasma sintering. *Scripta Materialia*. https://doi.org/10.1016/j.scriptamat.2

016.01.010

Chen, M., McCauley, J. W., & Hemker, K. J. (2003). Shock-induced localized amorphization in boron carbide. *Science*. https://doi.org/10.1126/science.1080819

Chen, M. W., McCauley, J. W., LaSalvia, J. C., & Hemker, K. J. (2005). Microstructural characterization of commercial hot-pressed boron carbide ceramics. *Journal of the American Ceramic Society*. https://doi.org/10.1111/j.1551-2916.2005.00346.x

Emin, D., & Aselage, T. L. (2005). A proposed boron-carbide-based solid-state neutron detector. *Journal of Applied Physics*. https://doi.org/10.1063/1.1823579

Hitchcock, D., Livingston, R., & Liebenberg, D. (2015). Improved understanding of the spark plasma sintering process. *Journal of Applied Physics*. https://doi.org/10.1063/1.4919814

Larsson, P., Axén, N., & Hogmark, S. (2000). Improvements of the microstructure and erosion resistance of boron carbide with additives. *Journal of Materials Science*. https://doi.org/10.1023/A:1004888522607

Lee, H., Speyer, R. F., & Hackenberger, W. S. (2002). Sintering of boron carbide heat-treated with hydrogen. *Journal of the American Ceramic Society*. https://doi.org/10.1111/j.1151-2916.2002.tb00420.x

Liu, J., Cardamone, A., Potter, T., German, R. M., & Semel, F. J. (2000). Liquid phase sintering of iron-carbon alloys with boron additions. *Powder Metallurgy*. https://doi.org/10.1179/pom.2000.43.1.57

Luo, S. D., Yang, Y. F., Schaffer, G. B., & Qian, M. (2013). The effect of a small addition of boron on the sintering densification, microstructure and mechanical properties of powder metallurgy Ti-7Ni alloy. *Journal of Alloys and Compounds*. https://doi.org/10.1016/j.jallcom.2012.12.068

Reed, J. S. (1994). *Principles of Ceramics Processing* (2nd Ed). John Wiley & Sons Inc.

Roy, T. K., Subramanian, C., & Suri, A. K. (2006). Pressureless sintering of boron carbide. *Ceramics International*. https://doi.org/10.1016/j.ceramint.2005.02.008

Shen, Z., & Nygren, M. (2005). Microstructural prototyping of ceramics by kinetic engineering: Applications of spark plasma sintering. *Chemical Record*. https://doi.org/10.1002/tcr.20043

Thévenot, F. (1990). Boron carbide-A comprehensive review. *Journal of the European Ceramic Society*. https://doi.org/10.1016/0955-2219(90)90048-K

W.D. Kingery, H.K. Bowen, D. R. U. (1975). *Introduction to Ceramics* (2nd Ed). John Wiley & Sons Inc.

Zhang, Z. H., Liu, Z. F., Lu, J. F., Shen, X. B., Wang, F. C., & Wang, Y. D. (2014). The sintering mechanism in spark plasma sintering - Proof of the occurrence of spark discharge. *Scripta Materialia*. https://doi.org/10.1016/j.scriptamat.2014.03.011

APPENDIX

Table 1. Properties of the samples in this work

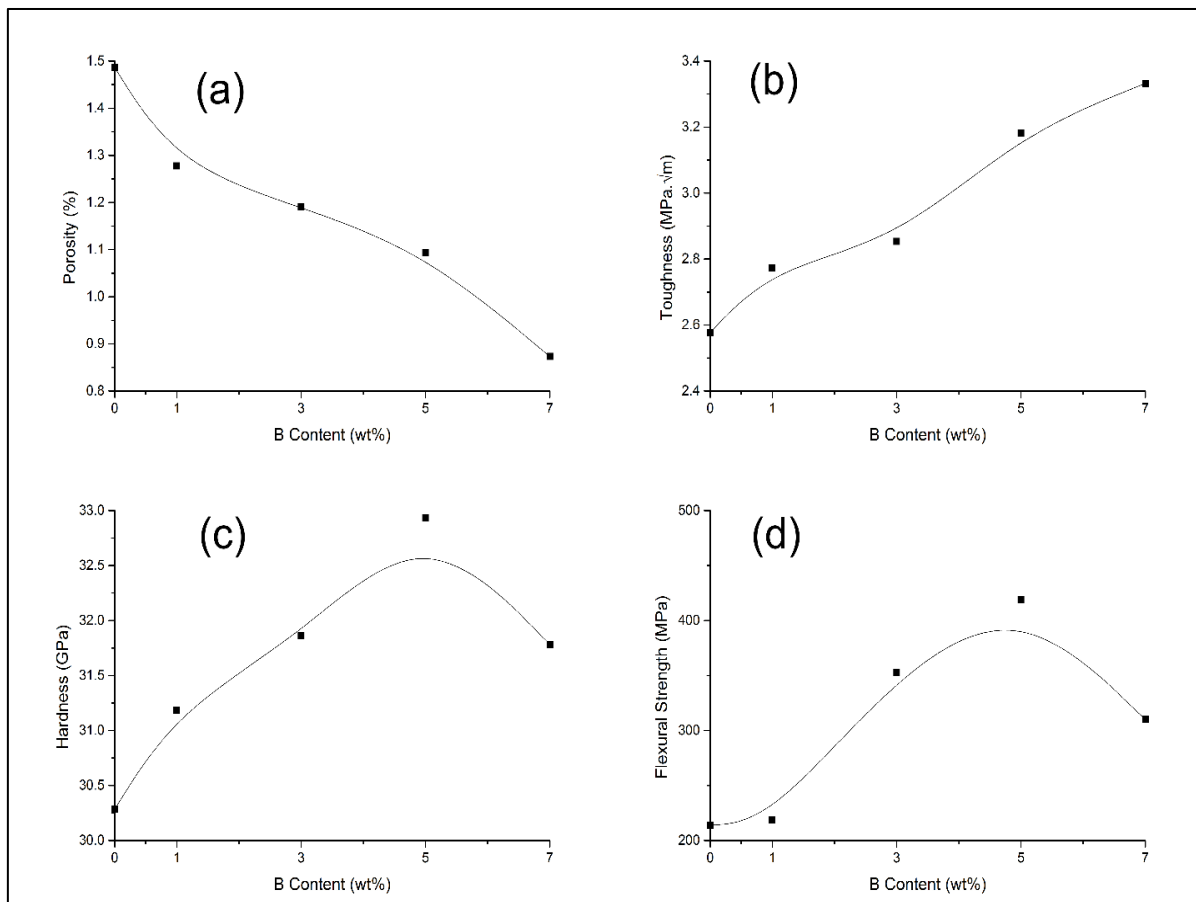| Amount of B (wt%)	Apparent Porosity (P,%)	Hardness (GPa)	Fracture Toughness (MPa√m)	Flexure Strength (MPa)
0	1.49	30.29	2.58	213.7
1	1.28	31.19	2.77	218.6
3	1.19	31.86	2.85	352.5
5	1.09	32.93	3.18	419.3
7	0.87	31.78	3.33	309.9

Source: Processed by Authors, 2020.

Figure 6. Plotted porosity (a), fracture toughness (b), hardness (c), and flexural strength (d) of the samples
Source: Processed by Authors, 2020.